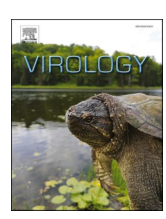
ELSEVIER

Contents lists available at ScienceDirect

Virology

journal homepage: www.elsevier.com/locate/virology



Production of cytoplasmic type citrus leprosis virus-like particles by plant molecular farming

Oscar A. Ortega-Rivera ^{a,b}, Veronique Beiss ^{a,b}, Elizabeth O. Osota ^{a,b}, Soo Khim Chan ^{a,b}, Sweta Karan ^{a,b}, Nicole F. Steinmetz ^{a,b,c,d,e,f,*}

- ^a Department of NanoEngineering, University of California-San Diego, La Jolla, CA, 92039, USA
- ^b Center for Nano-ImmunoEngineering, University of California-San Diego, La Jolla, CA, 92039, USA
- ^c Institute for Materials Discovery and Design, University of California-San Diego, La Jolla, CA, 92039, USA
- ^d Department of Bioengineering, University of California-San Diego, La Jolla, CA, 92039, USA
- ^e Department of Radiology, University of California-San Diego, La Jolla, CA, 92039, USA
- ^f Moores Cancer Center, University of California-San Diego, La Jolla, CA, 92039, USA

ABSTRACT

Many plant virus-like particles (VLPs) utilized in nanotechnology are 30-nm icosahedrons. To expand the VLP platforms, we produced VLPs of Cytoplasmic type citrus leprosis virus (CiLV-C) in *Nicotiana benthamiana*. We were interested in CiLV-C because of its unique bacilliform shape (60–70 nm \times 110–120 nm). The CiLV-C capsid protein (p29) gene was transferred to the pTRBO expression vector transiently expressed in leaves. Stable VLPs were formed, as confirmed by agarose gel electrophoresis, transmission electron microscopy and size exclusion chromatography. Interestingly, the morphology of the VLPs (15.8 \pm 1.3 nm icosahedral particles) differed from that of the native bacilliform particles indicating that the assembly of native virions is influenced by other viral proteins and/or the packaged viral genome. The smaller CiLV-C VLPs will also be useful for structure–function studies to compare with the 30-nm icosahedrons of other VLPs.

1. Introduction

Plant viruses are widely used as platform technologies and nanoparticles that can be repurposed and engineered for diverse applications, including the investigation of viral assembly mechanisms (Twarock and Stockley, 2019), the development of nanocontainers for catalysts or drugs (Steinmetz et al., 2020), precision farming (Chariou et al., 2019; Cao et al., 2015) as well as veterinary (Hoopes et al., 2018) and human health (Chung et al., 2022). Plant viruses and their non-infectious counterparts, the virus-like particles (VLPs) are particularly promising as vaccine and immunotherapy platforms. For example, a COVID-19 vaccine candidate based on tobacco mosaic virus (TMV) was produced by Kentucky BioScience International, LLC (Royal et al., 2021). Indeed, much research and many applications have focused on use of TMV, which is a 300×18 nm hollow nanotube in its native state but can also form spherical nanoparticles upon heat transformation (Atabekov et al., 2011). Many different icosahedral plant viruses have been studied and engineered, many of which form 30-nm particles with T=3 or pT=3symmetry. Examples include cowpea mosaic virus (CPMV) (Lizotte et al., 2016), cowpea chlorotic mottle virus (CCMV) (Brasch et al., 2017), cucumber mosaic virus (CuMV) (Nuzzaci et al., 2007), red clover necrotic mottle virus (RCNMV) (Cao et al., 2015), and hibiscus chlorotic ringspot virus (HCRSV) (Ren et al., 2007). Nanotechnology has taught us that the material properties and in vivo fate of nanoparticles are governed by their physiochemical characteristics, size and shape (Toy et al., 2014). We therefore searched the International Committee on Taxonomy of Viruses (ICTV) database for plant viruses with different morphologies. This led us to cytoplasmic type citrus leprosis virus (CiLV-C), which forms bacilliform particles with dimensions of 60–70 nm \times 110–120 nm.

CiLV-C causes citrus leprosis, a viral disease of citrus crops that is prevalent in South and Central America (Locali-Fabris et al., 2006). The disease is transmitted when plants are infested with mites (*Brevipalpus* spp.) and is caused by at least three viruses (CiLV-C being one of them), which establish non-systemic infections characterized by chlorotic lesions with necrotic ringspots on leaves, and chlorotic lesions and/or browning of fruits (Locali-Fabris et al., 2006). The disease results in fruit loss, stem dieback and in severe infestations can even kill citrus trees. The combined cost of yield losses and chemical control measures for the prevention of mite infestations come to more than US\$100 millions per year (Rodrigues, 2000). CiLV-C is the most widely distributed of the three viruses and is the type member of the genus *Cilevirus*, family

^{*} Corresponding author. Department of NanoEngineering, University of California-San Diego, La Jolla, CA, 92039, USA. *E-mail address:* nsteinmetz@ucsd.edu (N.F. Steinmetz).

Kitaviridae (Freitas-Astua et al., 2018; Chabi-Jesus et al., 2021). Its bacilliform particles surround a positive-sense ssRNA genome in two segments, each featuring a 5' cap and 3' polyadenylate tail. The first segment (RNA1) contains two open reading frames (ORFs) encoding a multi-domain replication-associated protein and the capsid protein, p29 (Locali-Fabris et al., 2006; Pascon et al., 2006; Leastro et al., 2018). The second segment (RNA2) contains four ORFs encoding p15, which is required for the formation of vesicles in the ER (Leastro et al., 2018), the p61 glycoprotein with roles in the remodeling of the ER and Golgi body (Leastro et al., 2018; Kuchibhatla et al., 2014), the movement protein p32, and the integral membrane protein p24, which is also involved in viral replication and assembly in the ER and may function as a matrix protein (Leastro et al., 2018).

To learn more about the assembly of CiLV-C, we transiently expressed the p29 capsid protein in *Nicotiana benthamiana* plants in an attempt to generate VLPs. Unlike native viruses, VLPs lack any genomic material and are therefore unable to replicate, but they are often structurally similar to the parental virus and still capable of interacting with target cells (Zeltins, 2013). Therefore, CiLV-C VLPs would make a useful addition to the viral nanoparticle platforms currently being investigated. The availability of VLPs would also allow us to work on the development of more effective and less environmentally hazardous control measures to prevent citrus leprosis.

2. Methods

2.1. Expression and purification of CiLV-C VLPs

The wild-type CiLV-C p29 sequence (UniProt: Q1KZ58) was reverse translated and codon optimized for N. benthamiana using SnapGene. The cDNA was synthesized by Genscript Biotech and transferred from the source vector pUC57-mini_P29_CiLVC to the PacI-AvrII site of vector pTRBO (Addgene #80082) (Lindbo, 2007). The insert was verified by colony PCR using primers TRBO-f (5'-GAT GAT TCG GAG GCT ACT GTC-3') and P29-r 5'-CAG AAG GAC CAG GTT GAA GTT G-3'). The reaction was heated to 95 °C for 30 s followed by 30 cycles of 95 °C for 30 s, 60 °C for 30 s and 68 °C for 30 s, and a final elongation step at 68 °C for 5 min. The presence of the insert was confirmed by digestion with the restriction enzymes PacI and AvrII (New England Biolabs) followed by 1% (w/v) agarose gel electrophoresis. Further, the identity of the p29 gene was validated by sequencing using Eurofins Genomics (Fig. S1). Sequencing was performed on a PCR product obtained using pTRBO vector specific forward and reverse primers: TRBO 5'-GATGATTCGGAGGCTACTGTC-3' and TRBO RP 5'-CTACCT-CAAGTTGCAGGACCG-3'. Sequences data were analyzed by BlastN and BlastX analysis and CLUSTAL OMEGA sequence alignment.

Then Agrobacterium tumefaciens strain GV3101 (Gold Biotechnology) was transformed by electroporation and cultured at 28 °C in YEB medium (5 g/L beef extract, 1 g/L yeast extract, 5 g/L peptone, 5 g/L sucrose, 0.5 g/L MgCl₂) supplemented with 50 µg/ml kanamycin, 30 µg/ml gentamycin and 25 µg/ml rifampicin. Bacterial cultures were resuspended in infiltration buffer (10 mM MES pH 5.5, 10 mM MgCl₂, 2% (w/v) sucrose, 200 µM acetosyringone) and the OD_{600nm} was adjusted to 1. The suspension was incubated for 4 h at room temperature before adding 0.01% (v/v) Silwet L-77 immediately prior to vacuum infiltration. Leaves of 6-week-old N. benthamiana plants were vacuum infiltrated as previously described (Plesha et al., 2009) with an absolute pressure of 0.23 atm for 3 min before release. The infiltrated leaves were allowed to air dry under a fume hood for 1 h and the plants were then maintained at 24 °C and 60% humidity for 7 days with a 16-h photoperiod (10,000 lux). The leaves were harvested and stored at -80 °C.

The purification protocol was adapted from ref. (Murray et al., 2019). VLPs were recovered from $\sim \! 100$ g of agroinfiltrated tissue by pulverization and homogenization in three volumes (300 mL) of cold 0.1 M sodium phosphate buffer (pH 7.0) containing 2% (w/v) polyvinylpolypyrrolidone (Sigma-Aldrich). The cell lysate was filtered

through Miracloth to remove debris and centrifuged $(12,000\times g,20$ min, $4\,^{\circ}$ C). The supernatant was supplemented with 0.2 M NaCl and 8% (w/v) PEG (MW 8000) and stirred overnight at $4\,^{\circ}$ C. The solution was centrifuged $(14,000\times g,15$ min, $4\,^{\circ}$ C) and the pellet was redissolved in 50 ml 10 mM sodium phosphate buffer (pH 7.0) overnight. The next day, the solution was centrifuged $(12,000\times g,15$ min, $4\,^{\circ}$ C) and the cleared supernatant was pelleted by ultracentrifugation $(169,000\times g,3$ h, $4\,^{\circ}$ C). The pellet was resuspended in 2 ml 0.1 M sodium phosphate buffer (pH 7.0) overnight at $4\,^{\circ}$ C. Finally, the VLPs were purified by ultracentrifugation on a 30% sucrose cushion $(133,000\times g,3$ h, $4\,^{\circ}$ C). The light scattering VLP band was collected, pelleted by ultracentrifugation $(169,000\times g,3$ h, $4\,^{\circ}$ C), and the pellet was resuspended in 0.1 M sodium phosphate buffer (pH 7.0). The total protein concentration was determined using a BCA assay (Thermo Fisher Scientific).

2.2. Electrophoretic characterization of VLPs

The VLPs were characterized by denaturing sodium dodecyl sulfate polyacrylamide gel electrophoresis (SDS-PAGE) and agarose gel electrophoresis. For SDS-PAGE, we loaded 10-µg and 20-µg samples of total protein per lane on NuPAGE 4–12% gels and fractionated them for 37 min at 200 mV. The gels were stained with GelCode Blue Safe Protein Stain (Thermo Fisher Scientific). For agarose gel electrophoresis, 20-µg samples of total protein were loaded onto 1.2% (w/v) agarose gels and fractionated for 1 h at 80 mV. For nucleic acid identification the gel was stained with GelRed (Gold Biotechnology) and for protein identification the gel was stained with Coomassie Brilliant Blue. All gels were imaged using the ProteinSimple FluorChem R imaging system.

2.3. Transmission electron microscopy

Carbon-coated copper negative stain grids were glow-discharged for 30 s (easiGlow) before adding 10-µl samples of total protein, incubating for 2 min and blotting away excess liquid. The grids were washed twice in Milli-Q water before applying two lots of 10 µl 2% (w/v) uranyl acetate, leaving the stain for 30 s each time before blotting. The grids were air dried and analyzed on a JEOL JEM-1400 series 120 kV Transmission Electron Microscope. The size of the CiLV-C VLPs was determined analyzing three images at different magnifications (60,000 \times , 80,000 \times and 100,000 \times) and measuring the diameter of 100 particles from five random fields (20 particles/field) in each image. The diameter of the 300 particles in total was presented as a frequency–size distribution histogram and the polydispersity index (PDI) was calculated as follows:

 $PDI = (standard deviation / mean diameter size)^2$

2.3.1. Size exclusion chromatography

CiLV-C VLPs were analyzed by size exclusion chromatography (SEC) using an AKTA Pure system fitted with a Superose 6 Increase 10/300~GL column (GE Healthcare). Samples (500 μg total protein) were analyzed at a flow rate of 0.5 ml/min using 0.1 M sodium phosphate buffer (pH 7.0).

3. Results and discussion

The codon-optimized CiLV-C p29 sequence was synthesized by GenScript Biotech and provided in vector pUC57-mini_P29_CiLVC. We transferred the *p29* ORF to the pTRBO vector, which contains the TMV replicase and movement protein genes (Lindbo, 2007) and is widely used for the overexpression of recombinant proteins in plants (Fig. 1a). The recombinant vector pTRBO_P29_CiLVC was introduced into *A. tumefaciens* strain GV3101 by electroporation, and the presence of the insert was confirmed by colony PCR (Fig. 1b) and a diagnostic restriction assay, which yielded a product of ~813 bp in addition to the >10-kb

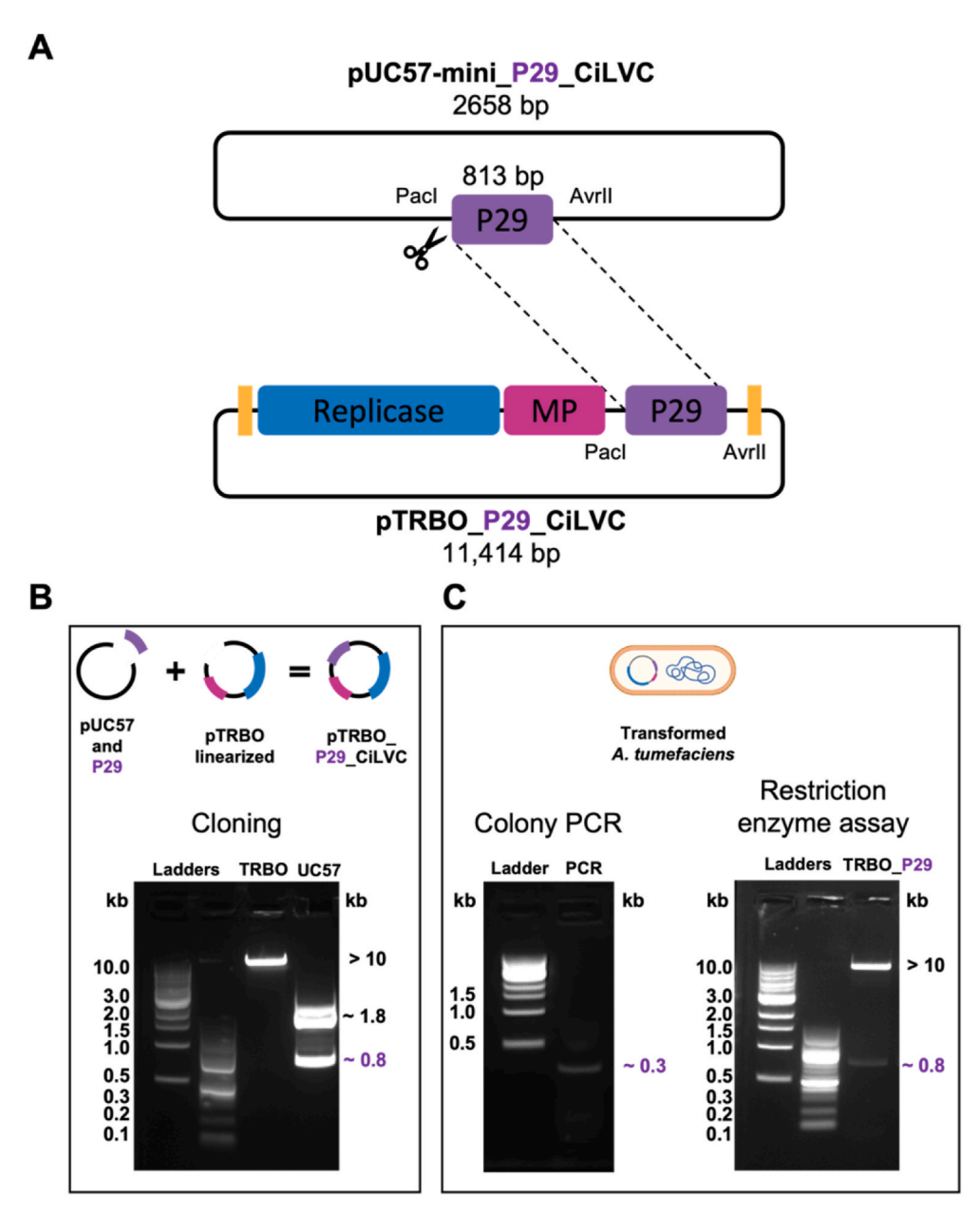


Fig. 1. Cloning of the CiLV-C p29 gene in a plant expression vector. (A) The p29 gene was transferred from its source vector pUC57-mini P29 CiLVC to the pTRBO (tobacco mosaic virus RNA-based overexpression) vector using the restriction enzymes PacI and AvrII, yielding the final vector pTRBO P29 CiLVC. (B) Digestion of pUC57-mini_P29_CiLVC with PacI and AvrII, releasing the p29 gene as an 813-bp fragment. The same enzymes were used to linearize pTRBO to allow unidirectional ligation. (C) Following the electroporation of tumefaciens strain GV3101 with pTRBO_P29_CiLVC, the presence of the insert was confirmed by colony PCR to vield a 307-bp product, and by a diagnostic restriction digest to release the entire 813-bp insert along with the >10-kb linearized pTRBO backbone. Lastly, sequencing confirmed the identity of the p29 gene (Fig. S1). Cloning and expression of the CiLV-C p29 gene.

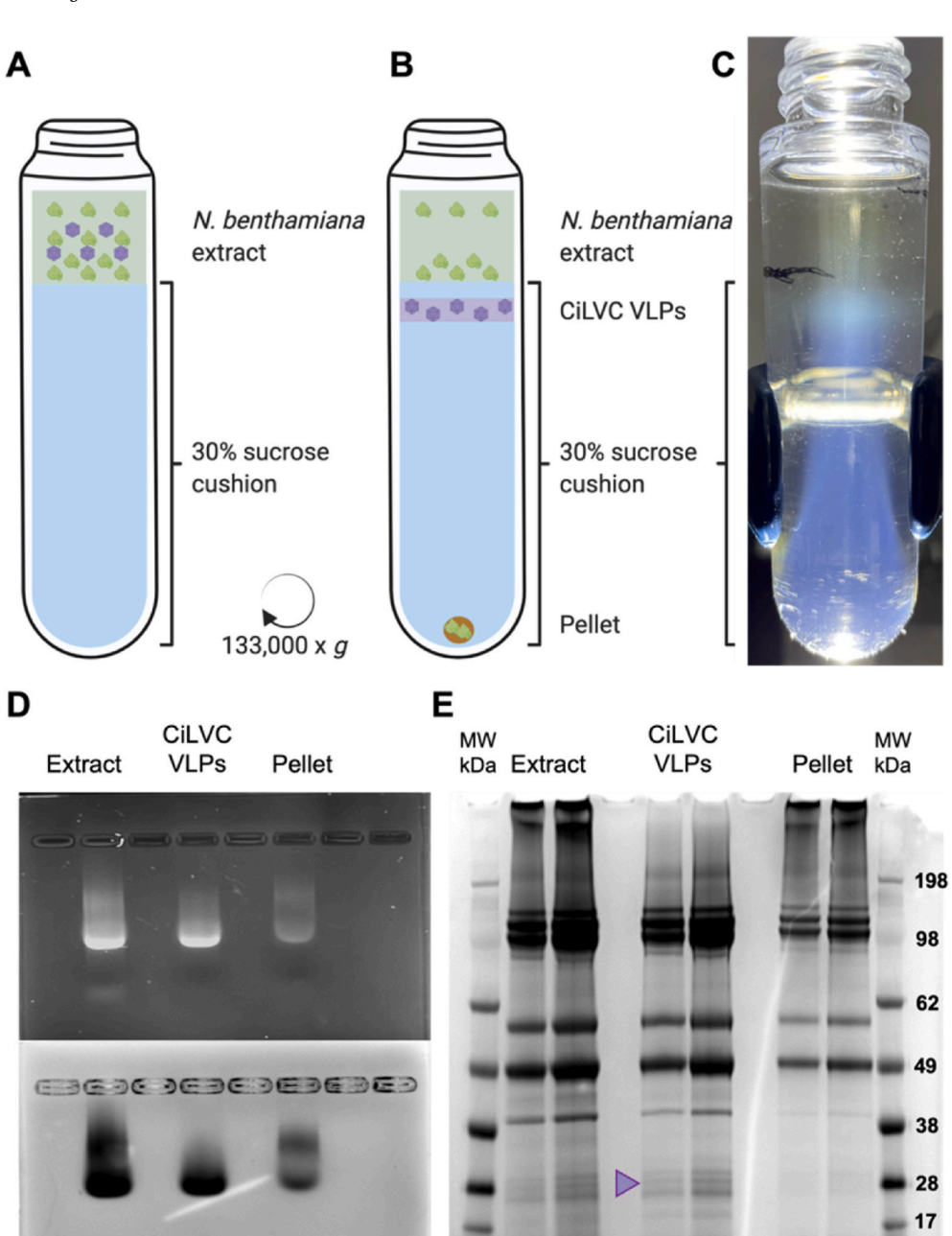
linearized pTRBO backbone (Fig. 1c). Finally, sequencing confirmed the identity of the *p29* gene (Fig. S1).

The leaves of 6-week-old *N. benthamiana* plants were vacuum infiltrated with the suspension of *A. tumefaciens* and left to express the p29 protein for 7 days. VLPs were then recovered from leaf extracts by ultracentrifugation over a 30% sucrose cushion (Fig. 2a–c). Agarose gel electrophoresis showed that extracts before and after ultracentrifugation contained comigrating nucleic acid and protein bands (Fig. 2d). VLPs lack genomic RNA, but often package random host RNA molecules based on nonspecific electrostatic interactions with the nucleic acid backbone (Mohsen et al., 2018), given the absence of a common packaging motif. We will investigate the nature of these captured RNA molecules in future work. SDS-PAGE under denaturing conditions confirmed the presence of the 29-kDa capsid protein in the crude extract before ultracentrifugation, and in the VLP band, but not in the pellet (Fig. 2e).

TEM analysis of the VLP band as well as pellet was performed confirming the presence of VLPs only in the light scattering band, denoted as the VLP band (Fig. S2). Once we confirmed the presence of VLPs in the light scattering band, the samples were further analyzed by SEC which

revealed one major peak at \sim 15 mL (Fig. 3a). Fractions were analyzed by SDS-PAGE revealing a 29-kDa protein the in major peak fraction (Fig. 3b). Finally, TEM imaging of the major peak fraction also confirmed the presence of icosahedral particles (Fig. 3c). The original morphological description of CiLV-C referred to short bacilliform particles (60–70 nm \times 110–120 nm) in the cisternae of the ER, as well as electron-dense viroplasms distributed in the cytoplasm (Kitajima et al., 1972). However, the analysis of TEM images revealed an icosahedral morphology with T = 1 symmetry (Fig. 3c) and the VLPs were also smaller in size than the native particles (15.8 \pm 1.3 nm) with a PDI of 0.006 (Fig. S3).

Our goal was to produce bacilliform VLPs larger than the typical 30-nm icosahedrons formed by other plant viruses. Although the CiLV-C VLPs did not assemble into the anticipated bacilliform particles, the icosahedral particles with T = 1 symmetry were smaller than usual (\sim 15 nm) and offer an opportunity to test for size-specific behavior during cell uptake and in vivo trafficking. VLPs that self-assemble from capsid proteins expressed in microbes, animal cells, plant cells or cell-free systems often resemble the structure of the parent virus, but this



> P29 protein

Fig. 2. Purification and analysis of CiLV-C VLPs. (A-C) Schematic illustration of the sucrose cushion ultracentrifugation step. (A) The N. benthamiana leaf extract was loaded onto the 30% sucrose cushion. (B) After ultracentrifugation, the CiLV-C VLPs formed a band at the top of the sucrose cushion and most plant proteins either remained in the aqueous zone or formed a pellet. (C) Image of a tube after ultracentrifugation showing the CiLV-C VLP band. (D) Analysis of 20 µg of total protein from the crude extract (left), the VLP band (middle) and the pellet (right) by 1.2% agarose gel electrophoresis. The top image shows nucleic acid staining (GelRed) and the bottom image shown protein staining (Coomassie Brilliant Blue) confirming the comigration of protein and nucleic acid in intact VLPs. (E) Denaturing SDS-PAGE in 4-12% polyacrylamide gels of 10 and 20 μg of total protein from the crude extract (left), the VLP band (middle) and the pellet (right), indicating the presence of p29 in the crude extract and VLPs but not the pellet. Size and morphology of the CiLV-C VLPs.

is not always the case. For example, in contrast to most members of the *Alfamovirus* genus, many strains of alfalfa mosaic virus (AlMV) are composed of bacilliform particles, but expressing the coat protein in *Escherichia coli* produces icosahedral particles with T = 1 symmetry similar to those we observed for CiLV-C (Yusibov et al., 1996; Choi and Loesch-Fries, 1999). This is likely to reflect the absence of viral genomic RNA, which normally coordinates the assembly of coat protein subunits. Indeed. AlMV can form particles with various morphologies, including bacilliform, icosahedral and long tubular structures resembling the cross-section of the icosahedral capsid (with or without icosahedral end caps) depending on the presence/absence of nucleic acids (Fukuyama et al., 1983) and the specific type: heterologous virus genome, calf thymus DNA, yeast total RNA, or poly(A) RNA (Hull, 1970; Driedonks et al., 1977). These morphologies can also be replicated by limited

CiLVC VLPs

Plant proteins

trypsin digestion (Bol et al., 1974) and by coat protein mutants that influence the formation of coat protein dimers (as the basic unit of capsid assembly) and the choice between the formation of pentamers or hexamers (Choi and Loesch-Fries, 1999; Kumar et al., 1997). Furthermore, to restore the bacilliform of CiLV-C, co-expression of additional structural proteins may be necessary. The integral membrane protein p24, has been implicated to play a role as a matrix protein (Leastro et al., 2018), and thus may be required for assembly of the bacilliform. We also note that it may also be possible that bacilliform particles might be present but are less stable or are present at too low titers and possibly do not elute in the expected purification fractions.

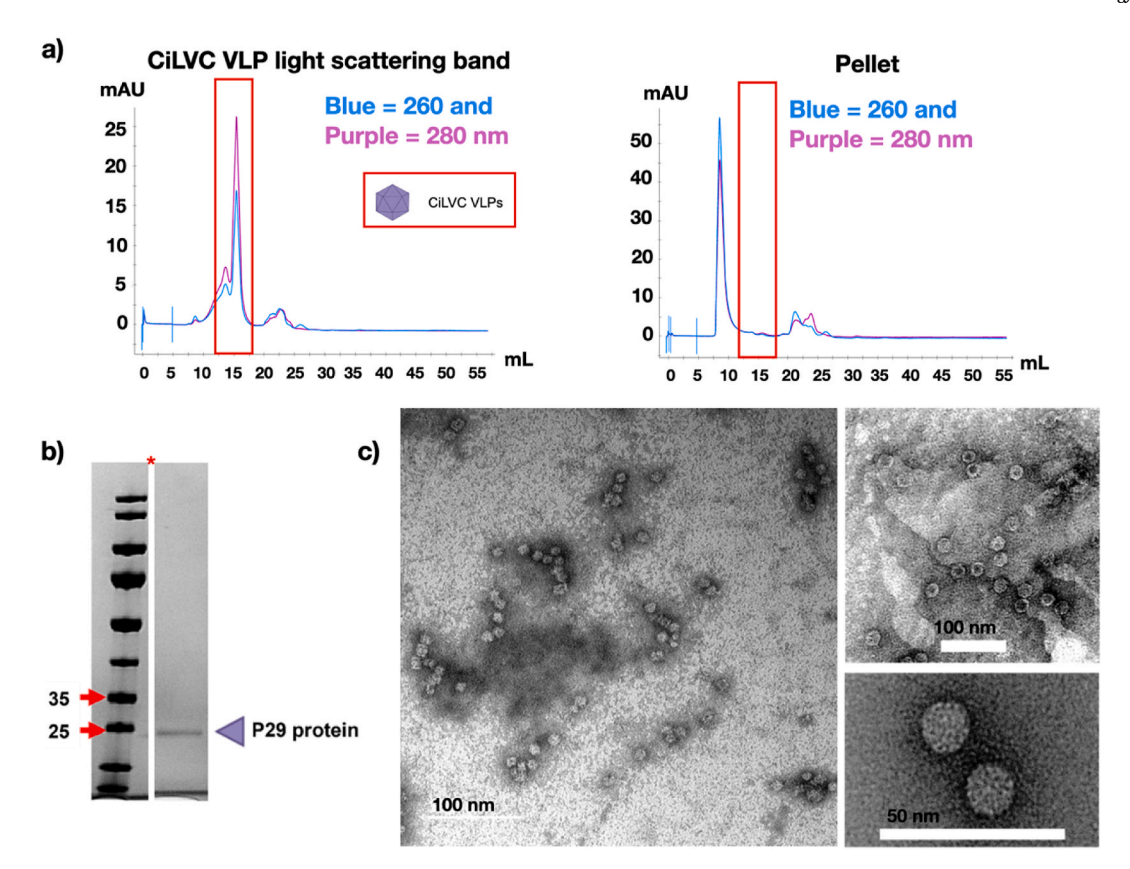


Fig. 3. Purification of CiLV-C VLPs by size exclusion chromatography (SEC) and characterization of the fractions. (A) SEC revealed one major peak at ~ 15 mL for the light scattering band (CiLV-C VLPs band in Fig. 2b) – larger, possibly aggregates were observed when the pellet fraction was subjected to SEC analysis. (B) SDS-PAGE analysis in 4–12% polyacrylamide gels under denaturing conditions reveals the presence of the p29 protein in the major peak fraction. (C) TEM images of the major peak fraction showing pure CiLV-C VLPs (49,000 \times , scale bar = 100 nm; and 128,000 \times , scale bar = 50 nm).

4. Conclusion

We expressed the CiLV-C p29 capsid protein in *N. benthamiana* and confirmed that it self-assembles into stable VLPs, albeit differing in size and morphology from the native CiLV-C particles. Such differences are often observed when some of the components required to assemble native particles are missing (in this case, the most likely candidates are the native RNA1 and RNA2, but potentially also one or more of the five additional CiLV-C proteins). The production of CiLV-C VLPs provides insight into the assembly mechanism and may facilitate the development of more effective countermeasures against citrus leprosis based on the direct inhibition of the viral replication cycle. CiLV-C VLPs could also be developed as delivery platforms for drugs, vaccines, and imaging reagents.

CRediT authorship contribution statement

Oscar A. Ortega-Rivera: Conceptualization, Methodology, Validation, Formal analysis, Investigation, Writing – original draft, Visualization. Veronique Beiss: Methodology, Validation, Formal analysis, Investigation. Elizabeth O. Osota: Investigation. Soo Khim Chan: Investigation. Sweta Karan: Investigation, Visualization. Nicole F. Steinmetz: Conceptualization, Validation, Resources, Data curation, Writing – review & editing, Visualization, Supervision, Project administration, Funding acquisition.

Declaration of competing interest

The authors declare that they have no known competing financial interests or personal relationships that could have appeared to influence the work reported in this paper.

Dr. Steinmetz is a co-founder of, has equity in, and has a financial interest with Mosaic ImmunoEngineering Inc. Dr. Steinmetz serves as Director, Board Member, and Acting Chief Scientific Officer, and paid consultant to Mosaic. The other authors declare no potential conflict of interest.

Acknowledgments

This work was supported in part by a grant from the National Institute of Health (U01 CA218292, R21 AI161306, R01 CA224605 to N.F. S.) and the National Science Foundation through the UC San Diego Materials Research Science and Engineering Center (DMR-2011924 to N.F.S.). O.A.O.-R. acknowledges the UC MEXUS-CONACYT Postdoctoral Fellowship 2019–2020 number FE-19-58. E.O.O. was supported by the NIH 2T32 CA153915-06A1 institutional training grant through the Cancer Research in Nanotechnology San Diego Fellowship. Some Figures were made in part using Biorender.com. The authors thank Andrea Monroy Borrego (UC San Diego) for help with plant maintenance and agroinfiltration.

Appendix A. Supplementary data

Supplementary data to this article can be found online at https://doi.org/10.1016/j.virol.2022.11.004.

References

Atabekov, J., Nikitin, N., Arkhipenko, M., Chirkov, S., Karpova, O., 2011. Thermal transition of native tobacco mosaic virus and RNA-free viral proteins into spherical nanoparticles. J. Gen. Virol. 92 (Pt 2), 453–456.

- Bol, J.F., Kraal, B., Brederode, F.T., 1974. Limited proteolysis of alfalfa mosaic virus: influence on the structural and biological function of the coat protein. Virology 58 (1), 101–110.
- Brasch, M., Putri, R.M., de Ruiter, M.V., Luque, D., Koay, M.S., Caston, J.R., Cornelissen, J.J., 2017. Assembling enzymatic cascade pathways inside virus-based nanocages using dual-tasking nucleic acid tags. J. Am. Chem. Soc. 139 (4), 1512–1519.
- Cao, J., Guenther, R.H., Sit, T.L., Lommel, S.A., Opperman, C.H., Willoughby, J.A., 2015. Development of abamectin loaded plant virus nanoparticles for efficacious plant parasitic nematode control. ACS Appl. Mater. Interfaces 7 (18), 9546–9553.
- Chabi-Jesus, C., Ramos-Gonzalez, P.L., Postclam-Barro, M., Fontenele, R.S., Harakava, R., Bassanezi, R.B., Moreira, A.S., Kitajima, E.W., Varsani, A., Freitas-Astua, J., 2021. Molecular epidemiology of citrus leprosis virus C: a new viral lineage and phylodynamic of the main viral subpopulations in the Americas. Front. Microbiol. 12. 641252.
- Chariou, P.L., Dogan, A.B., Welsh, A.G., Saidel, G.M., Baskaran, H., Steinmetz, N.F., 2019. Soil mobility of synthetic and virus-based model nanopesticides. Nat. Nanotechnol. 14 (7), 712–718.
- Choi, J., Loesch-Fries, L.S., 1999. Effect of C-terminal mutations of alfalfa mosaic virus coat protein on dimer formation and assembly in vitro. Virology 260 (1), 182–189.
- Chung, Y.H., Church, D., Koellhoffer, E.C., Osota, E., Shukla, S., Rybicki, E.P., Pokorski, J.K., Steinmetz, N.F., 2022. Integrating plant molecular farming and materials research for next-generation vaccines. Nat. Rev. Mater. 7 (5), 372–388.
- Driedonks, R.A., Krijgsman, P.C., Mellema, J.E., 1977. Alfalfa mosaic virus protein polymerization. J. Mol. Biol. 113 (1), 123–140.
- Freitas-Astua, J., Ramos-Gonzalez, P.L., Arena, G.D., Tassi, A.D., Kitajima, E.W., 2018.

 Brevipalpus-transmitted viruses: parallelism beyond a common vector or convergent evolution of distantly related pathogens? Curr. Opin. Virol. 33, 66–73.
- Fukuyama, K., Abdel-Meguid, S.S., Johnson, J.E., Rossmann, M.G., 1983. Structure of a T = 1 aggregate of alfalfa mosaic virus coat protein seen at 4.5 A resolution. J. Mol. Biol. 167 (4), 873–890.
- Hoopes, P.J., Wagner, R.J., Duval, K., Kang, K., Gladstone, D.J., Moodie, K.L., Crary-Burney, M., Ariaspulido, H., Veliz, F.A., Steinmetz, N.F., Fiering, S.N., 2018. Treatment of canine oral melanoma with nanotechnology-based immunotherapy and radiation. Mol. Pharm. 15 (9), 3717–3722.
- Hull, R., 1970. Studies on alfalfa mosaic virus. 3. Reversible dissociation and reconstitution studies. Virology 40 (1), 34–47.
- Kitajima, E.W., Muller, G.W., Costa, A.S., Yuki, W., 1972. Short, rod-like particles associated with Citrus leprosis. Virology 50 (1), 254–258.
- Kuchibhatla, D.B., Sherman, W.A., Chung, B.Y., Cook, S., Schneider, G., Eisenhaber, B., Karlin, D.G., 2014. Powerful sequence similarity search methods and in-depth manual analyses can identify remote homologs in many apparently "orphan" viral proteins. J. Virol. 88 (1), 10–20.
- Kumar, A., Reddy, V.S., Yusibov, V., Chipman, P.R., Hata, Y., Fita, I., Fukuyama, K., Rossmann, M.G., Loesch-Fries, L.S., Baker, T.S., Johnson, J.E., 1997. The structure of alfalfa mosaic virus capsid protein assembled as a T=1 icosahedral particle at 4.0-A resolution. J. Virol. 71 (10), 7911–7916.
- Leastro, M.O., Kitajima, E.W., Silva, M.S., Resende, R.O., Freitas-Astua, J., 2018. Dissecting the subcellular localization, intracellular trafficking, interactions, membrane association, and topology of citrus leprosis virus C proteins. Front. Plant Sci. 9, 1299.

- Lindbo, J.A., 2007. TRBO: a high-efficiency tobacco mosaic virus RNA-based overexpression vector. Plant Physiol. 145 (4), 1232–1240.
- Lizotte, P.H., Wen, A.M., Sheen, M.R., Fields, J., Rojanasopondist, P., Steinmetz, N.F., Fiering, S., 2016. In situ vaccination with cowpea mosaic virus nanoparticles suppresses metastatic cancer. Nat. Nanotechnol. 11 (3), 295–303.
- Locali-Fabris, E.C., Freitas-Astua, J., Souza, A.A., Takita, M.A., Astua-Monge, G., Antonioli-Luizon, R., Rodrigues, V., Targon, M., Machado, M.A., 2006. Complete nucleotide sequence, genomic organization and phylogenetic analysis of Citrus leprosis virus cytoplasmic type. J. Gen. Virol. 87 (Pt 9), 2721–2729.
- Mohsen, M.O., Gomes, A.C., Vogel, M., Bachmann, M.F., 2018. Interaction of viral capsid-derived virus-like particles (VLPs) with the innate immune system. Vaccines 6
- Murray, A.A., Sheen, M.R., Veliz, F.A., Fiering, S.N., Steinmetz, N.F., 2019. In situ vaccination of tumors using plant viral nanoparticles. Methods Mol. Biol. 2000, 111–124
- Nuzzaci, M., Piazzolla, G., Vitti, A., Lapelosa, M., Tortorella, C., Stella, I., Natilla, A., Antonaci, S., Piazzolla, P., 2007. Cucumber mosaic virus as a presentation system for a double hepatitis C virus-derived epitope. Arch. Virol. 152 (5), 915–928.
- Pascon, R.C., Kitajima, J.P., Breton, M.C., Assumpcao, L., Greggio, C., Zanca, A.S., Okura, V.K., Alegria, M.C., Camargo, M.E., Silva, G.G., Cardozo, J.C., Vallim, M.A., Franco, S.F., Silva, V.H., Jordao Jr., H., Oliveira, F., Giachetto, P.F., Ferrari, F., Aguilar-Vildoso, C.I., Franchiscini, F.J., Silva, J.M., Arruda, P., Ferro, J.A., Reinach, F., da Silva, A.C., 2006. The complete nucleotide sequence and genomic organization of Citrus Leprosis associated Virus, Cytoplasmatic type (CiLV-C). Virus Gene. 32 (3), 289–298.
- Plesha, M.A., Huang, T.K., Dandekar, A.M., Falk, B.W., McDonald, K.A., 2009. Optimization of the bioprocessing conditions for scale-up of transient production of a heterologous protein in plants using a chemically inducible viral amplicon expression system. Biotechnol. Prog. 25 (3), 722–734.
- Ren, Y., Wong, S.M., Lim, L.Y., 2007. Folic acid-conjugated protein cages of a plant virus: a novel delivery platform for doxorubicin. Bioconjugate Chem. 18 (3), 836–843.
- Rodrigues, J.C.V., 2000. Relações patógeno-vetor-planta no sistema leprose dos citros. Centro de Energia Nuclear na Agricultura, Universidade de São Paulo.
- Royal, J.M., Simpson, C.A., McCormick, A.A., Phillips, A., Hume, S., Morton, J., Shepherd, J., Oh, Y., Swope, K., DeBeauchamp, J.L., Webby, R.J., Cross, R.W., Borisevich, V., Geisbert, T.W., Demarco, J.K., Bratcher, B., Haydon, H., Pogue, G.P., 2021. Development of a SARS-CoV-2 vaccine candidate using plant-based manufacturing and a tobacco mosaic virus-like nano-particle. Vaccines 9 (11).
- Steinmetz, N.F., Lim, S., Sainsbury, F., 2020. Protein cages and virus-like particles: from fundamental insight to biomimetic therapeutics. Biomater. Sci. 8 (10), 2771–2777.
- Toy, R., Peiris, P.M., Ghaghada, K.B., Karathanasis, E., 2014. Shaping cancer nanomedicine: the effect of particle shape on the in vivo journey of nanoparticles. Nanomedicine 9 (1), 121–134.
- Twarock, R., Stockley, P.G., 2019. RNA-mediated virus assembly: mechanisms and consequences for viral evolution and therapy. Annu. Rev. Biophys. 48, 495–514.
- Yusibov, V., Kumar, A., North, A., Johnson, J.E., Loesch-Fries, L.S., 1996. Purification, characterization, assembly and crystallization of assembled alfalfa mosaic virus coat protein expressed in Escherichia coli. J. Gen. Virol. 77 (Pt 4), 567–573.
- Zeltins, A., 2013. Construction and characterization of virus-like particles: a review. Mol. Biotechnol. 53 (1), 92–107.